Increased accuracy of ligand sensing by receptor internalization

Gerardo Aquino and Robert G. Endres
Division of Molecular Biosciences and Centre for Integrated Systems Biology at Imperial College, Imperial College London, SW7 2AZ London, United Kingdom

(Received 25 August 2009; revised manuscript received 21 December 2009; published 8 February 2010)

Many types of cells can sense external ligand concentrations with cell-surface receptors at extremely high accuracy. Interestingly, ligand-bound receptors are often internalized, a process also known as receptor-mediated endocytosis. While internalization is involved in a vast number of important functions for the life of a cell, it was recently also suggested to increase the accuracy of sensing ligand as the overcounting of the same ligand molecules is reduced. Here we show, by extending simple ligand-receptor models to out-of-equilibrium thermodynamics, that internalization increases the accuracy with which cells can measure ligand concentrations in the external environment. Comparison with experimental rates of real receptors demonstrates that our model has indeed biological significance.

DOI: 10.1103/PhysRevE.81.021909 PACS number(s): 87.10.Mn, 87.16.dj, 87.18.Tt

I. INTRODUCTION

Biological cells can sense and respond to various chemicals in their environment. However, the precision with which a cell can measure the concentration of a specific ligand is negatively affected by many sources of noise [1–5]. Most noticeable is external noise from the random arrival of ligand molecules at the cell-surface receptors by diffusion. Nonetheless several examples exist in which measurements are performed with surprisingly high accuracy. In bacterial chemotaxis, for instance, fast moving bacteria such as *Escherichia coli* can respond to changes in concentration as low as 3.2 nM [6]. This value is remarkable since cells have only about 1 s between "tumbles" to evaluate the ligand concentration [7]. Furthermore, this concentration value corresponds to only about three ligand molecules in the volume of the cell, assumed to be 1 fl, suggesting single molecule detection. High accuracy is observed also in spatial sensing by single cell eukaryotic organisms. Best characterized is the slime mold *Dictyostelium discoideum*, which is able to sense a concentration difference of 1–5 % across the cell diameter [8], as well as *Saccharomyces cerevisiae* (budding yeast), able to orient growth in a gradient of α- pheromone mating factor down to estimated 1% receptor occupancy difference across the cell [9]. Spatial sensing is also efficiently performed by lymphocytes, neutrophils, and other cells of the immune system [10], as well as by growing synaptic and tumor cells.

Previously, the fundamental physical limits to the accuracy of sensing as set by ligand diffusion have been calculated [11–15]. Recent work based on simplifying models indicates that, if a cell effectively acts as an absorber of ligand, the accuracy is significantly increased [16]. Such an increase in accuracy can be explained with the fact that absorption prevents ligand molecules from unbinding the receptors. Hence, the same ligand molecule can only be counted once by a receptor, avoiding a source of measurement uncertainty. However, whether cells with realistic receptors can act as absorbers and increase the accuracy of sensing is unknown.

Motivated by these observations, in this paper we analyze the role of receptor-mediated endocytosis, i.e., the internalization of either bound or unbound receptors from the cell membrane into the cell interior, often observed in eukaryotic cells [17,18]. Internalization of ligand-bound receptors effectively leads to the absorption of ligand molecules and is therefore expected to draw the cell nearer to the physical limit of the *perfect absorber* [16]. Using simple models for the ligand-receptor dynamics, we find that the effect of receptor-mediated endocytosis indeed increases the accuracy of sensing ligand concentration if internalization of ligand competes with ligand unbinding. Comparison of our results to the available literature of experimental rate constants shows that receptors often work in this limit, indicating biological relevance of our results.

The paper is organized as follows: In Sec. II we review the results regarding the accuracy of sensing for a single immobile receptor without internalization. In Sec. III, we study the role of internalization using a model of ligand-receptor dynamics with internalization. While ligand-receptor binding and unbinding are described by equilibrium thermodynamics, as previously developed in Refs. [12,20], internalization clearly introduces nonequilibrium thermodynamics into the problem. We consider the limit of fast diffusion, i.e., when the coupling to diffusion of ligand can be neglected, as well as the general case both near and far from equilibrium. This general case deals with the reduction of rebinding of previously bound ligand molecules by receptor internalization and hence represents the main result of the work. In Sec. IV we analyze the results obtained in Sec. III and connect to receptors from the biological literature. We conclude with final comments and discussion. Appendixes A and B are devoted to an alternative approach leading to the same results derived in the main text.

II. REVIEW OF THE SINGLE RECEPTOR

In this section we review previous results for a single immobile receptor without internalization. Details of the method will be provided in Sec. III. As depicted in Fig. 1, such a receptor can bind and release ligand with rates $k_+\bar{c}$ and k_-, respectively. The kinetics for the occupancy $n(t)$ of the receptor are therefore given by

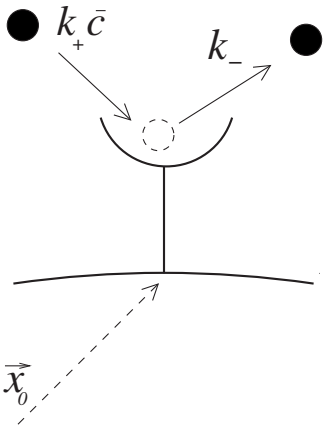

FIG. 1. Single receptor, immobile at position $\vec{x}_0$, binds and unbinds ligand with rates $k_+\bar{c}$ and k_-, respectively.

$$\frac{\partial n(t)}{\partial t} = k_+\bar{c}[1-n(t)] - k_-n(t), \tag{1}$$

where the concentration of ligand $c(\vec{x},t)=\bar{c}$ is assumed uniform and constant. The steady-state solution for the receptor occupancy is given by

$$\bar{n} = \frac{\bar{c}}{\bar{c}+K_D}, \tag{2}$$

with $K_D=k_-/k_+$ as the ligand dissociation constant. The rates of binding and unbinding are related to the (negative) free energy of binding through detailed balance

$$\frac{k_+\bar{c}}{k_-} = e^{F/T}, \tag{3}$$

with T as the temperature in energy units. In the limit of very fast ligand diffusion, i.e., when a ligand molecule is immediately removed from the receptor after unbinding, the dynamics of the receptor is effectively decoupled from the diffusion of ligand molecules and hence diffusion does not need to be included explicitly.

Following Bialek and Setayeshgar [12], the accuracy of sensing is obtained by applying the fluctuation dissipation theorem (FDT) [19], which relates the spectrum of the fluctuations in occupancy to the linear response to a perturbation in the receptor binding energy. Furthermore at equilibrium the fluctuations in occupancy can be directly related to the uncertainty in ligand concentration using Eq. (2). For a measurement performed on a time scale τ much larger than the correlation time of the binding and unbinding events, the fluctuations of the occupancy $\langle(\delta n)^2\rangle$ are obtained from the zero-frequency spectrum divided by τ. Using $\langle(\delta n)^2\rangle$, one then obtains the uncertainty in measuring ligand concentration $\bar{c}$ [12,20],

$$\frac{\langle(\delta c)^2\rangle_\tau}{\bar{c}^2} = \frac{2}{k_+\bar{c}(1-\bar{n})\tau} \to \frac{1}{2\pi D_3\bar{c}s\tau}, \tag{4}$$

where the right-hand side is obtained for diffusion-limited binding [20], i.e., when $k_+\bar{c}(1-\bar{n})\to 4\pi\bar{c}D_3s$, with D_3 as the diffusion constant and s as the dimension of the (spherical) receptor. Equation (4) shows that the accuracy of sensing is limited by the random binding and unbinding of ligand.

In the case where diffusion of ligand is slow, ligand binding to the receptor is affected by diffusion [12]. The kinetics of the receptor occupancy and ligand concentration are described by

$$\frac{\partial n(t)}{\partial t} = k_+c(\vec{x}_0,t)[1-n(t)] - k_-n(t), \tag{5a}$$

$$\frac{\partial c(\vec{x},t)}{\partial t} = D_3\nabla^2c(\vec{x},t) - \delta(\vec{x}-\vec{x}_0)\frac{\partial n(t)}{\partial t}, \tag{5b}$$

where $\vec{x}_0$ indicates the position of the receptor and $\delta(\vec{x}-\vec{x}_0)$ is a Dirac delta function centered at the receptor location. The last term in the second equation describes a sink or source of ligand at $\vec{x}_0$, corresponding to ligand-receptor binding or unbinding, respectively. Analogous to fast diffusion, Eq. (5) has steady-state solutions $\bar{c}$ (independent of D_3) and $\bar{n}$ given by Eq. (2).

Following a similar procedure as in the previous case, the accuracy of sensing is given by [12,20]

$$\frac{\langle(\delta c)^2\rangle_\tau}{\bar{c}^2} = \frac{2}{k_+\bar{c}(1-\bar{n})\tau} + \frac{1}{\pi s D_3\bar{c}\tau} \tag{6a}$$

$$\to \frac{3}{2\pi s D_3\bar{c}\tau}, \tag{6b}$$

where the first term on the right-hand side of Eq. (6a) is the same as in Eq. (4), while the second term is the increase in uncertainty due to diffusion. This term accounts for the additional measurement uncertainty from rebinding of previously bound ligand to the receptor. For diffusion-limited binding, one obtains Eq. (6b) [20].

Comparison of Eqs. (4) and (6) shows that removal of previously bound ligand by fast diffusion increases the accuracy of sensing since the same ligand molecule is never measured more than once.

III. EFFECT OF RECEPTOR INTERNALIZATION

Here, we consider the case of receptor internalization. As depicted in Fig. 2, receptors at $\vec{x}=\vec{x}_0$ can bind and unbind ligand with given rates. Furthermore, a bound receptor can be internalized at rate k_i, while an unbound receptor can be internalized at rate k_i^0. Hence, the kinetics of the fractions of occupied receptors $n(t)$ and unoccupied receptors $m(t)$ are given by

$$\frac{\partial n(t)}{\partial t} = k_+\bar{c}m(t) - (k_- + k_i)n(t), \tag{7a}$$

$$\frac{\partial m(t)}{\partial t} = -k_+\bar{c}m(t) - k_i^0m(t) + k_-n(t) + k_r. \tag{7b}$$

Imposing a single receptor at $\vec{x}=\vec{x}_0$ at any time via

$$n(t) + m(t) = 1, \tag{8}$$

Eq. (7b) becomes redundant. As shown in Fig. 3, this condition implies that an internalized receptor is immediately re-

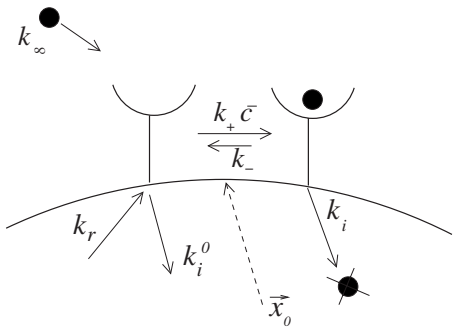

FIG. 2. Receptor with internalization. In addition to ligand binding and unbinding described in Fig. 1, the receptor is internalized at rate k_i, if occupied, and at rate k_i^0, if unoccupied. The internalized ligand is degraded. An unoccupied receptor is delivered to membrane with rate k_r.

placed by a new unoccupied receptor with rate $k_r(t) = k_i^0 m(t) + k_i n(t)$. Furthermore, rate k_∞ of incoming ligand compensates for internalized ligand.

A. Limit of fast diffusion

We first consider the case of fast diffusion, i.e., when ligand unbound from the receptor is immediately removed. In this case the kinetics for the occupancy $n(t)$ of the single receptor is described by

$$\frac{\partial n(t)}{\partial t} = k_+\bar{c}[1-n(t)] - (k_- + k_i)n(t) = k_+\bar{c}[1-n(t)] - \kappa_- n(t), \tag{9}$$

where $\kappa_- = k_- + k_i$ is the combined rate of unbinding and internalization. The steady-state solution for the receptor occupancy is given by

$$\bar{n}_i = \frac{\bar{c}}{\bar{c} + \kappa_-/k_+} = \frac{\bar{c}}{\bar{c} + K_M}, \tag{10}$$

where $K_M = \kappa_-/k_+$ is a Michael-Menten-type constant and subscript i is used to indicate the steady-state value for the occupancy of the receptor in presence of internalization [cf. Eq. (2)].

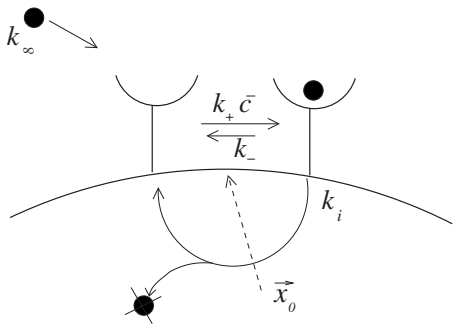

FIG. 3. Single receptor with internalization. Similar to Fig. 2 except that the delivery of receptor to the membrane is adjusted, so that Eq. (8) is fulfilled. This corresponds to an instantaneous replacement (round arrow) of the internalized receptor by a new receptor via the endocytosis machinery.

While Eq. (9) could be solved immediately by analogy to Eq. (1), we adopt here, for the fast diffusion case, the method of the effective temperature, which allows us to solve the general case in Sec. III B. Similar to the equilibrium case, at the nonequilibrium steady state the rates can formally be related to the binding free energy

$$\frac{k_+\bar{c}}{\kappa_-} = \frac{k_+\bar{c}}{k_-\left(1 + \frac{k_i}{k_-}\right)} = \frac{e^{F/T}}{1 + k_i/k_-} = e^{F/T_e}, \tag{11}$$

where we introduced the effective temperature

$$T_e = \frac{T}{1 - \frac{\ln(1 + k_i/k_-)}{\ln(k_+\bar{c}/k_-)}}. \tag{12}$$

Hence, the effective temperature maps the nonequilibrium steady state to an effective equilibrium, allowing the generalization of the FDT to out-of-equilibrium phenomena [21–24] with applications in modeling biological processes [25]. Conceptually, an effective temperature larger than the environment temperature ($T_e > T$) corresponds to a decrease in the receptor occupancy, approximately reflecting internalization in the nonequilibrium steady state.

In order to calculate the spectrum of the fluctuations in receptor occupancy, we follow Refs. [12,20] and consider small fluctuations around the stationary solution

$$n(t) = \bar{n}_i + \delta n(t).$$

In order to apply the generalized FDT (GFDT), we introduce fluctuations in the conjugate variable of the receptor occupancy, i.e., the free energy F, via fluctuations of the binding and unbinding rates,

$$\frac{\delta F}{T_e} = \frac{\delta k_+}{k_+} - \frac{\delta \kappa_-}{\kappa_-}, \tag{13}$$

where we approximate T_e as a parameter.

Linearization of Eq. (9) leads to

$$\frac{\partial[\delta n(t)]}{\partial t} = -(k_+\bar{c} + \kappa_-)\delta n(t) + k_+\bar{c}(1-\bar{n}_i)\frac{\delta F(t)}{T_e}, \tag{14}$$

where we used Eq. (13) to replace the fluctuations in the rate constants with fluctuations in the free energy, as well as steady-state solution [Eq. (10)].

Fourier transforming Eq. (14) yields the susceptibility

$$\hat{\chi}(\omega) = \frac{\delta\hat{n}(\omega)}{\delta\hat{F}(\omega)} = \frac{1}{T_e}\frac{k_+\bar{c}(1-\bar{n}_i)}{(k_+\bar{c} + \kappa_-) - i\omega}, \tag{15}$$

describing the linear response of the receptor occupancy to a perturbation in the free energy. We now use the GFDT to calculate the spectrum $S_n(\omega) = \langle|\delta n(\omega)|^2\rangle$ of the fluctuations in $n(t)$,

$$S_n(\omega) = \frac{2T_e}{\omega}\mathrm{Im}[\hat{\chi}(\omega)] = \frac{2k_+\bar{c}(1-\bar{n}_i)}{(k_+\bar{c}+\kappa_-)^2+\omega^2} = 2\langle(\delta n)^2\rangle\frac{\tau_C}{1+(\omega\tau_C)^2}, \quad (16)$$

where the correlation time $\tau_C=(k_+\bar{c}+\kappa_-)^{-1}$ and the total variance

$$\langle(\delta n)^2\rangle = \int_{-\infty}^{+\infty}\frac{d\omega}{2\pi}S_n(\omega) = \frac{k_+\bar{c}(1-\bar{n}_i)}{k_+\bar{c}+\kappa_-} = \bar{n}_i(1-\bar{n}_i) \quad (17)$$

have been introduced. Using Eq. (10), we calculate the uncertainty in ligand concentration from fluctuations in occupancy

$$\delta c = \frac{(\bar{c}+K_M)^2}{K_M}\delta n = \frac{K_M}{(1-\bar{n}_i)^2}\delta n = \frac{\bar{c}}{\bar{n}_i(1-\bar{n}_i)}\delta n. \quad (18)$$

From Eq. (18) the normalized variance can be obtained,

$$\frac{\langle(\delta c)^2\rangle}{\bar{c}^2} = \frac{1}{\bar{n}_i(1-\bar{n}_i)}, \quad (19)$$

corresponding to an instantaneous measurement.

In the more realistic case, in which a measurement is performed during an averaging time $\tau \gg \tau_C$, the error in the occupancy is linked to the low frequency spectrum via

$$\langle(\delta n)^2\rangle_\tau \simeq \frac{S_n(0)}{\tau} = \frac{2\bar{n}_i^2(1-\bar{n}_i)}{k_+\bar{c}\tau}. \quad (20)$$

Using Eqs. (18) and (20), the accuracy of sensing is given by

$$\frac{\langle(\delta c)^2\rangle_\tau}{\bar{c}^2} = \frac{2}{k_+\bar{c}(1-\bar{n}_i)\tau} \to \frac{1}{2\pi D_3\bar{c}s\tau}. \quad (21)$$

Equation (21) is identical to the result in Eq. (4) without internalization except that $\bar{n}_i<\bar{n}$ due to internalization. In fact, the removal of unbound ligand by fast diffusion at equilibrium is equivalent to removal of bound ligand by internalization at the nonequilibrium steady state. This equivalence can be readily seen from Eq. (9), which is indistinguishable from simple unbinding with rate $\kappa_-=k_-+k_i$. Hence, the effective temperature applied here is in fact exact.

B. Solution near equilibrium

When considering ligand diffusion, the above procedure still applies with the exception that the concentration of ligand is allowed to vary due to binding and unbinding. The kinetics of the receptor occupancy and ligand concentration is described by

$$\frac{\partial n(t)}{\partial t} = k_+c(\vec{x}_0,t)[1-n(t)] - \kappa_-n(t), \quad (22a)$$

$$\frac{\partial c(\vec{x},t)}{\partial t} = D_3\nabla^2c(\vec{x},t) - \delta(\vec{x}-\vec{x}_0)\left[\frac{\partial n(t)}{\partial t} + k_in(t)\right] + k_\infty\delta(\vec{x}-\vec{x}_\infty), \quad (22b)$$

where $\kappa_-=k_-+k_i$ is used as before. Furthermore, a source of ligand with rate k_∞ is considered at location $\vec{x}_\infty$ so as to compensate the loss of ligand molecules due to internalization.

We note that the steady-state solution for the concentration is not spatially uniform but is depleted near the receptor due to internalization. This leads to the anomaly that we mathematically evaluate the rate of binding using the ligand concentration at $\vec{x}_0$ in Eq. (22a), while physically the diffusive flux and hence binding of ligand are determined by the ligand concentration $\bar{c}$ far away from the receptor (see Sec. III C). This is remedied by linearizing the ligand concentration around $\bar{c}$ in the following. Furthermore, Eq. (8) is again assumed valid, and therefore an additional equation describing the unoccupied receptor fraction $m(t)$ with rates k_i^0 and k_r is redundant.

Linearizing Eqs. (22a) and (22b) leads to

$$\frac{\partial[\delta n(t)]}{\partial t} = k_+(1-\bar{n}_i)\delta c(\vec{x}_0,t) - (k_+\bar{c}+\kappa_-)\delta n(t) + \delta k_+(t)\bar{c}(1-\bar{n}_i) - \bar{n}_i\delta\kappa_-, \quad (23a)$$

$$\frac{\partial[\delta c(\vec{x},t)]}{\partial t} = D_3\nabla^2\delta c(\vec{x},t) - \delta(\vec{x}-\vec{x}_0)\left[\frac{\partial[\delta n(t)]}{\partial t} + k_i\delta n(t)\right]. \quad (23b)$$

By applying the quasiequilibrium picture with the effective temperature T_e introduced in Sec. III A, we use Eq. (13) to introduce fluctuations in the free energy and obtain

$$\frac{\partial[\delta n(t)]}{\partial t} = k_+(1-\bar{n}_i)\delta c(\vec{x}_0,t) - (k_+\bar{c}+\kappa_-)\delta n(t) + \kappa_-\bar{n}_i\frac{\delta F}{T_e}, \quad (24a)$$

$$\frac{\partial[\delta c(\vec{x},t)]}{\partial t} = D_3\nabla^2\delta c(\vec{x},t) - \delta(\vec{x}-\vec{x}_0)\left[\frac{\partial[\delta n(t)]}{\partial t} + k_i\delta n(t)\right]. \quad (24b)$$

Fourier transforming Eqs. (24a) and (24b), we obtain

$$\delta\hat{c}(\vec{q},\omega) = e^{i\vec{q}\cdot\vec{x}_0}\frac{i\omega-k_i}{D_3q^2-i\omega}\delta\hat{n}(\omega), \quad (25)$$

which can be inverse-Fourier transformed in $\vec{x}_0$,

$$\delta\hat{c}(\vec{x}_0,\omega) = (i\omega-k_i)\delta\hat{n}(\omega)\int\frac{d^3q}{(2\pi)^3}\frac{1}{D_3q^2-i\omega}. \quad (26)$$

Inserting Eq. (26) in Fourier-transformed Eq. (24a), we obtain

$$\hat{\chi}(\omega) = \frac{\delta\hat{n}(\omega)}{\delta F(\omega)} = \frac{1}{T_e}\frac{\kappa_-\bar{n}_i}{k_+\bar{c}+\kappa_-+(k_i-i\omega)\Sigma_1(\omega)-i\omega}, \quad (27)$$

where $\Sigma_1(\omega)$ is given by

$$\Sigma_1(\omega) = \int \frac{d^3q}{(2\pi)^3} \frac{k_+(1-\bar{n}_i)}{D_3 q^2 - i\omega} = \int_0^\Lambda \frac{dq}{2\pi^2} \frac{q^2[k_+(1-\bar{n}_i)]}{D_3 q^2 - i\omega}$$
$$\overset{\omega\to 0}{=} \frac{k_+(1-\bar{n}_i)\Lambda}{2\pi^2 D_3} \simeq \frac{k_+(1-\bar{n}_i)}{2\pi D_3 s}. \tag{28}$$

Here $\Lambda \simeq \pi/s$ is a cutoff due to the finite size s of the receptor, introduced to regularize the integral in Eq. (28). As before, we apply the GFDT to derive the spectrum of the fluctuations $\delta\hat{n}(\omega)$,

$$S_n(\omega) = \frac{2T_e}{\omega}\mathrm{Im}[\chi(\omega)]$$
$$= \frac{2k_+\bar{c}(1-\bar{n}_i)[1+\Sigma_1(\omega)]}{[k_i\Sigma_1(\omega) + k_+\bar{c} + \kappa_-]^2 + \omega^2[1+\Sigma_1(\omega)]^2}, \tag{29}$$

where we used Eq. (27) for the susceptibility. In the realistic case, in which the measurement is time averaged over duration τ much larger than the correlation time of the fluctuations, the relevant part of the spectrum is the zero-frequency limit,

$$S_n(\omega \simeq 0) = \frac{2k_+\bar{c}(1-\bar{n}_i)[1+\Sigma_1(0)]}{[k_+\bar{c} + \kappa_- + k_i\Sigma_1(0)]^2}$$
$$= 2\langle(\delta n)^2\rangle \frac{[1+\Sigma_1(0)]\tau_C}{[1+k_i\Sigma_1(0)\tau_C]^2}$$
$$\simeq 2\langle(\delta n)^2\rangle[1+\alpha\Sigma_1(0)]\tau_C, \tag{30}$$

where $\alpha = 1 - 2k_i\tau_C < 1$ and higher order terms in $\Sigma_1(0)$ are neglected for sufficiently fast diffusion. As before, $\langle(\delta n)^2\rangle = \bar{n}_i(1-\bar{n}_i)$ and $\tau_C = (k_+\bar{c} + \kappa_-)^{-1}$.

Using Eq. (18), the normalized variance of the concentration is given by

$$\frac{\langle(\delta c)^2\rangle_\tau}{\bar{c}^2} = \frac{\langle(\delta n)^2\rangle_\tau}{[\bar{n}_i(1-\bar{n}_i)]^2} = \frac{1}{[\bar{n}_i(1-\bar{n}_i)]^2}\frac{S_n(0)}{\tau}, \tag{31}$$

where τ is the averaging time. Using Eq. (30) for the power spectrum, we finally obtain for the accuracy of sensing with ligand internalization and diffusion

$$\frac{\langle(\delta c)^2\rangle_\tau}{\bar{c}^2} = \frac{2}{k_+\bar{c}(1-\bar{n}_i)\tau} + \frac{\alpha}{\pi D_3 \bar{c} s \tau} \tag{32a}$$

$$\to \frac{1+2\alpha}{2\pi D_3 \bar{c} s \tau}. \tag{32b}$$

The following conclusions can be drawn by comparison with the result [Eq. (6)] without internalization. (i) Receptor internalization mainly reduces the second term in Eq. (6), demonstrating that internalization increases the accuracy of sensing by reducing the uncertainty from rebinding of previously bound ligand. The first term is only reduced by replacing $\bar{n}$ by $\bar{n}_i$, with $\bar{n}_i < \bar{n}$. (ii) In the limit $k_i \to 0$, $\alpha \to 1$, and the equilibrium result [Eq. (6)] without internalization is recovered. (iii) As Eq. (31) becomes unphysical in the limit of $k_i \to \infty$, i.e., does not approach Eq. (21) without rebinding, our result can only be regarded an approximation valid near equilibrium.

C. Comparison with perfect absorber

The perfect absorber is here defined as a receptor, which internalizes a ligand immediately once it is bound. Following Ref. [16], the accuracy of sensing can be calculated from the Poisson statistics of the number of binding events N in time τ,

$$\frac{\langle(\delta c)^2\rangle_\tau}{\bar{c}^2} = \frac{\langle(\delta N)^2\rangle}{\langle N^2\rangle} = \frac{1}{4\pi D_3 s \bar{c} \tau}, \tag{33}$$

obtained from the diffusive flux of ligand to an absorbing sphere of radius s. Comparison with Eq. (21) for diffusion-limited binding without rebinding shows that the perfect absorber is yet more accurate by a factor 2. This is due to the fact that the fluctuations in occupancy in Eq. (21) stem from the random binding *and* unbinding/internalization events, while the uncertainty in Eq. (33) solely stems from the random binding events (see also factor 2 in Eq. (A2), as well as Ref. [26] for further explanation).

IV. IMPLICATIONS FOR BIOLOGY

In Sec. III C we showed that internalization increases the accuracy of sensing by reducing the measurement uncertainty from rebinding of previously bound ligand. In this section we review some receptors of known rate constants. We specifically would like to determine if the rate of internalization k_i is fast enough, i.e., comparable to the unbinding rate k_-, in order to effectively increase the accuracy of sensing.

In Table I, we summarize experimental values for rate constants, including internalization, of various receptors. Most G-protein coupled receptors (GPCRs) undergo internalization [18]. The Ste2 receptor in haploid yeast cells of α-mating type is involved in α pheromone sensing and signal transduction, leading to cell polarization, "shmoo" formation, and mating. The folate receptor (FR) in *Dictyostelium*, likely a GPCR [27,28], is used to sense and hunt bacteria. (The folate-binding protein in mammalian cells is a diagnostic marker for various cancers, and its internalization is exploited for drug delivery into cancerous human cell [29].) However, the cAR1 receptor in *Dictyostelium*, used for sensing of cAMP under starvation, is not internalized [30]. The epidermal growth factor receptor (EGFR), a tyrosine kinase, is another important example of a receptor which is internalized [31]. This receptor is involved in cell growth, proliferation, and differentiation [31–33]. Another class of internalized receptors is involved in uptake. Transferrin receptor (TfR) is used for iron uptake from extracellular space and plays therefore an important role in blood cells [31]. Transferrin binds to TfR, is internalized, and releases its iron load through ion pump-induced pH reduction. The ligand-bound TfR is then recycled back to cell surface. Another example is the low density lipoprotein receptor (LDLR) [31]. When bound to LDL-cholesterol via adaptin, LDLR is inter-

TABLE I. Summary of experimental data for relevant receptor rates discussed in the main text.

Receptor	Function	k_- (min^{-1})	K_D (nM)	k_i (min^{-1})	k_i^0 (min^{-1})
	Chemotaxis:				
FR	Feeding	0.096[a]	20.0[a,b]	9.6×10^{-4} [c]	
Ste2	Mating	0.06[d]	22.1[d]	0.24[e]	0.024[e]
		0.0108[f]	6.0[f]	0.156[g]	0.0156[g]
EGFR[h]	Development	0.24	2.47	0.15	0.02
	Uptake:				
TfR[h]	Iron	0.09	29.8	0.6	0.6
LDLR[h]	Cholesterol	0.04	14.3	0.195	0.195
VtgR[h]	Vitellogenin	0.07	1300	0.108	0.108

[a]Reference [34].
[b]However, other values have been reported as well [41].
[c]This rate is measured for folate-binding protein in cancerous mice cells and not in *Dictyostelium* [29].
[d]Reference [35].
[e]Reference [36].
[f]Reference [37].
[g]Reference [38].
[h]Reference [31].

nalized via clathrin-coated vesicles [31]. Furthermore, the vitellogenin receptor (VtgR) is involved in oogenesis (egg formation) [31]. Once internalized, vitellogenin is turned into yolk proteins. Ligand-free receptors are recycled back to cell surface. Table I shows that in most cases k_i is of the same order or larger than k_-, except for FR, where internalization is much slower than the unbinding of the ligand from the receptor.

Figure 4 visualizes the contribution of internalization to the accuracy of sensing for the receptors from Table I. The faster the internalization, the larger the increase of the accuracy of sensing. However internalization can only reduce the

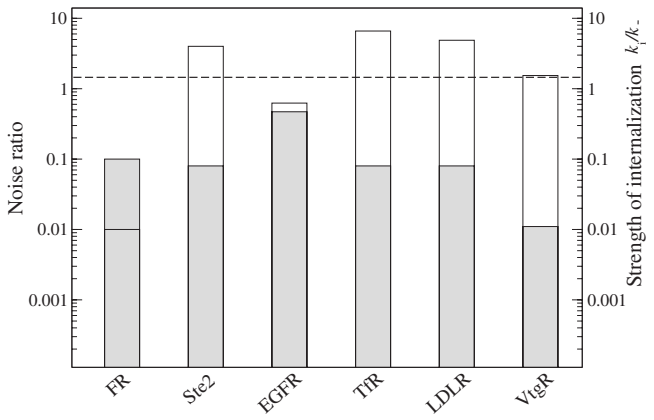

FIG. 4. Analysis of receptor rate data from Table I. (Filled bars) Noise ratio defined as the square root of the second (rebinding) term and the first (random binding and unbinding) in Eq. (6a). (Open bars) Strength of internalization, defined by ratio k_i/k_-. The dashed line indicates the noise ratio ($\sqrt{2}$) for diffusion-limited binding $[k_+\bar{c}(1-\bar{n})\to 4\pi\bar{c}D_3 s]$. Numerical values of the plot are provided in Appendix B.

second term in Eq. (6a) from rebinding of previously bound ligand, not the first term from random binding and unbinding. To illustrate the relative contribution of the two terms, we plot the square root of their ratio in Fig. 4 (filled bars). This shows that in most cases, in which internalization occurs, the noise ratio of the two terms is significant, ranging from few hundredths to order of unity. Hence, internalization can lead to a substantial increase in the accuracy of sensing. However, measured rate constants are substantially uncertain (see below) and diffusion coefficients of small ligand molecules range from 0.1 $\mu\text{m}^2/\text{s}$ in the synaptic cleft between neurons [39] to 1–10 $\mu\text{m}^2/\text{s}$ in blood [40] to 300 $\mu\text{m}^2/\text{s}$ in water [16]. In order to avoid this uncertainty in parameters, we also plot the upper limit of the noise ratio for diffusion-limited binding equal to $\sqrt{2}$ (dashed line in Fig. 4). Removal of the second noise term in this limit by internalization would increase the accuracy in Eq. (6b) by a factor of 3. In Fig. 4, we also show the strength of internalization, defined by the ratio of internalization and unbinding rates (open bars).

How reliable are the measured values for the rate constants? Rate constants are generally obtained through radioactive labeling of ligand, with the isotope choice targeted to each specific case (the isotope ^{125}I giving the most accurate measurements) [42]. In order to measure the unbinding and the binding rates, i.e., k_- and $k_+=k_-/K_D$, the receptors on the membrane must be separated by filtration or centrifugation from the soluble ligand. If the ligand-unbinding process is slow compared to separation, then the measurement of the amount of bound ligand through the radioactive label can be easily carried out; in the case of fast unbinding, measurements are less accurate. For the internalization rate, the ratio between the intensity at the surface and inside the cell is measured and from the slope of the time variation of this ratio, k_i is determined [43]. This method, though, does not

take into account recycling (diacytosis) of the receptor, which is a recurrent feature of the internalization process, also included in our model. These shortcomings, as well as the variability associated with different cell preparations, lead to a large error in the rate determination (~20%) [42] and variability between different measurements (20–90 %). Other measurement methods employed in experiments include protease sensitivity assays [44] and destination assays [45].

Many examples in fact suggest a direct relation between ligand internalization and the accuracy of sensing, measured by the sensitivity of cell polarization or cell movement in shallow chemical gradients. These include sensing of α factor by budding yeast [37,38], folate by *Dictyostelium* [27], and PDGF by fibroblasts [46]. Other examples relate to embryonic development. In zebrafish, primordial germ cells migrate toward chemokine SDF-1a that binds and activates the receptor CXCR4b. It was recently shown that ligand-induced CXCR4b internalization is required for precise arrival of germ cells at their target destination [47]. During *Drosophila* oogenesis, border cells perform directional migration [32]. EGFR, together with two other receptor tyrosine kinases, is the main guidance receptor. Recent work in this system provided compelling evidence that guided cell movement also requires spatial control of signaling events by endocytic dynamics [48,49].

V. DISCUSSION AND CONCLUSIONS

In this paper we analyzed the role of receptor internalization in the accuracy of sensing ligand concentration. By extending equilibrium single receptor models to nonequilibrium thermodynamics introduced by internalization, we derived expressions for the uncertainty in sensing ligand concentration. As expected, internalization of ligand-bound receptors makes the cell act similarly to an absorber and increases the accuracy of sensing. We then analyzed relevant experimental data, summarized in Table I, and concluded that, in most cases, the contribution of receptor internalization to the increase in accuracy of sensing is non-negligible. However, a perfect absorber is yet more accurate as its uncertainty only stems from random binding events, not from additional random unbinding *and* internalization events. Whether cells have developed mechanisms to approach the limit of the perfect absorber, e.g., by internalization, is not clear yet. However, since the accuracy of concentration sensing can always be improved by increasing the averaging time, one might expect that receptor internalization becomes increasingly important when time is of the essence. In addition to chemotaxis, embryonic development may be a biological system for which receptor internalization is important. Specifically, the Fgf8 morphogen, which regulates tissue differentiation and morphogenesis in zebrafish, forms exponential concentration gradients by diffusion and degradation, the latter being achieved precisely by receptor internalization [50]. However, based on our results, internalization may also be used for the accurate readout of the gradient in the short amount of time dictated by cell division.

Cells generally have many receptors to estimate external concentrations of chemicals, leading to a spatial averaging and consequently further increase in the accuracy of sensing. However, even the employment of many receptors cannot increase the accuracy of sensing beyond the physical limit of the perfect absorber [26]. In fact a cell only needs a relatively small number of receptors to achieve an accuracy comparable to the physical limit [7]. On the downside, if a cell uses many receptors, it needs to integrate this information in signaling pathways. If this process is fundamentally limited by noise as well, then this noise provides an upper limit on the overall estimation performance.

Although we analyzed the role of receptor internalization in increasing the accuracy of sensing, it is important to stress that internalization fulfills several other known purposes in cells [51]. Among them are (i) redistribution of receptors to different locations on the cell membrane, (ii) uptake of nutrients and chemicals, (iii) signaling by ligand in cell interior, and (iv) turning off persistent signal as part of adaptation. All these aspects would need to be considered to fully characterize the working of a receptor.

In order to derive the accuracy of sensing with internalization, we made a number of simplifying assumptions. In our model we neglected other possible sources of fluctuations such as fluctuations in receptor density in order to relate our results to the single immobile receptor. Furthermore, we introduced the effective temperature T_e to generalize the FDT to nonequilibrium thermodynamics. While T_e is well defined for well separated time scales, a potential time or frequency dependence of T_e [22–24] was neglected here. However, our nonequilibrium result with internalization is consistent with the equilibrium result in the fast diffusion limit. Removal of ligand by fast diffusion at equilibrium is equivalent to removal of bound ligand by internalization at the nonequilibrium steady state, providing confidence in our method.

Internalization is not the only mechanism, by which a cell can act as an absorber and increase its accuracy of sensing. Other potential mechanisms include enzymatic degradation of ligand at the cell surface, e.g., degradation of cAMP by mPDE in *Dictyostelium* and of α-mating pheromone by Bar1 in budding yeast [52,53]. Furthermore, at excitatory neural synapses, fast diffusion of AMPA receptors on the postsynaptic membrane surface has an important role in the sensing of neurotransmitter glutamate [54]. Ligand-bound desensitized receptors diffuse away and are replaced by fresh receptors, leading to fast recovery and readiness for the next action potential and release of neurotransmitter. By the same mechanism, the accuracy of sensing may be increased since ligand-bound receptors diffuse away and release ligand far away from region of signaling, thus preventing an overcounting of same ligand molecules [55].

ACKNOWLEDGMENTS

We thank Robert Insall, Luca Leuzzi, Yigal Meir, and Ned Wingreen for helpful discussions, any two anonymous referees for their helpful comments. We acknowledge financial support from Biotechnological and Biological Sciences Research Council Grant No. BB/G000131/1 and the Centre for Integrated Systems Biology at Imperial College.

APPENDIX A: LANGEVIN APPROACH

As an alternative derivation, here we provide the solution for the accuracy of sensing for internalization using a Langevin approach. We first consider fast diffusion. We start from Eq. (9) but add a noise term, $\xi_n(t)$,

$$\frac{\partial n(t)}{\partial t} = k_+\bar{c}[1-n(t)] - \kappa_- n(t) + \xi_n(t), \tag{A1}$$

where we assume

$$\langle|\hat{\xi}_n(\omega)|^2\rangle = k_+\bar{c}(1-\bar{n}_i) + \kappa_-\bar{n}_i = 2k_+\bar{c}(1-\bar{n}_i) \tag{A2}$$

due to Poisson statistics [56,57]. Linearizing and Fourier transforming Eq. (A1), assuming the rates k_+ and κ_- constant, leads to

$$\delta\hat{n}(\omega) = \frac{\hat{\xi}_n(\omega)}{k_+\bar{c} + \kappa_- - i\omega}. \tag{A3}$$

Hence, the power spectrum of the fluctuations in receptor occupancy is given by

$$S_n(\omega) = \langle|\delta\hat{n}(\omega)|^2\rangle = \frac{\langle|\hat{\xi}_n(\omega)|^2\rangle}{(k_+\bar{c}+\kappa_-)^2+\omega^2} = \frac{2k_+\bar{c}(1-\bar{n}_i)}{(k_+\bar{c}+\kappa_-)^2+\omega^2}, \tag{A4}$$

where in the last step the property [Eq. (A2)] was used. Equation (A4) is indeed equivalent to result (16) in the main text.

For the general solution, we start from Fourier-transformed Eqs. (24) and (26), i.e.,

$$(k_+\bar{c} + \kappa_- - i\omega)\,\delta\hat{n}(\omega) = k_+(1-\bar{n}_i)\,\delta\hat{c}(\vec{x}_0,\omega) + \hat{\xi}_n(\omega) \tag{A5}$$

and

$$\delta\hat{c}(\vec{x}_0,\omega) = \frac{(i\omega - k_i)}{k_+(1-\bar{n}_i)}\Sigma_1(\omega)\,\delta\hat{n}(\omega) + \hat{\xi}_c(\omega), \tag{A6}$$

respectively, where $\hat{\xi}_n(\omega)$ and $\hat{\xi}_c(\omega)$ are additive noise terms and $\Sigma_1(\omega)$ is given by Eq. (28). Inserting Eq. (A6) in Eq. (A5) and solving for $\delta\hat{n}(\omega)$ lead to

$$\delta\hat{n}(\omega) = \frac{\hat{\xi}_n(\omega) + k_+(1-\bar{n}_i)\hat{\xi}_c(\omega)}{k_+\bar{c} + \kappa_- + k_i\Sigma_1(\omega) - i\omega[1+\Sigma_1(\omega)]}, \tag{A7}$$

from which the following expression for $\langle|\delta n(\omega)|^2\rangle$ ensues

$$\langle|\delta\hat{n}(\omega)|^2\rangle = \frac{k_+^2(1-\bar{n}_i)^2\langle|\hat{\xi}_c(\omega)|^2\rangle + \langle|\hat{\xi}_n(\omega)|^2\rangle}{[k_+\bar{c}+\kappa_- + k_i\Sigma_1(\omega)]^2 + \omega^2[1+\Sigma_1(\omega)]^2}. \tag{A8}$$

In the limit $\omega\to 0$, using Eq. (A2) as in the previous case, we obtain

$$\langle|\delta\hat{n}(\omega)|^2\rangle \overset{\omega\to 0}{=} \frac{k_+^2(1-\bar{n}_i)^2\langle|\hat{\xi}_c(\omega)|^2\rangle + 2k_+\bar{c}(1-\bar{n}_i)}{[k_+\bar{c}+\kappa_- + k_i\Sigma_1(0)]^2}. \tag{A9}$$

Following [58], we set

$$\langle|\hat{\xi}_c(\omega)|^2\rangle \simeq S_c^{3D}(\omega\to 0) \sim \frac{\bar{c}}{D_3 s} \sim \frac{\Sigma_1(0)}{k_+(1-\bar{n}_i)} \tag{A10}$$

in Eq. (A9) and obtain for the power spectrum

$$\langle|\delta\hat{n}(\omega)|^2\rangle = \frac{2\langle(\delta n)^2\rangle[1+\Sigma_1(0)]\tau_C}{[1+k_i\Sigma_1(0)\tau_C]^2}. \tag{A11}$$

Equation (A11) is identical to result (30), obtained with the GFDT in main text.

APPENDIX B: NUMERICAL VALUES

In this section we provide the numerical values used for plotting Fig. 4. Noise ratio and internalization strengths are given by 0.1/0.01 (FR), 0.08/4 (Ste2), 0.47/0.625 (EGFR), 0.08/6.6 (TfR), 0.08/4.875 (LDLR), and 0.011/1.54 (VtgR). Specifically, to calculate the noise ratio, the first and the second terms in Eq. (6a) are given by (in units of τ) 2500/27.6 (FR), 4000/25.1 (Ste2), 1000/224 (EGFR), 2667/18.6 (TfR), 6000/38.72 (LDLR), and 3428/0.426 (VtgR). We have used $s=1$ nm, $\bar{n}=1/2$, i.e., setting $\bar{c}=K_D$ from Table I, and $D_3 = 1\ \mu\text{m}^2/\text{s}$.

[1] A. Raj and A. van Oudenaarden, Cell **135**, 216 (2008).
[2] R. C. Yu *et al.*, Nature (London) **456**, 755 (2008).
[3] M. S. Samoilov, G. Price, and A. P. Arkin, Sci. STKE **2006**, re17 (2006).
[4] T. Gregor *et al.*, Cell **130**, 153 (2007).
[5] V. Shahrezaei and P. S. Swain, Curr. Opin. Biotechnol. **19**, 369 (2008).
[6] H. Mao, P. S. Cremer, and M. D. Manson, Proc. Natl. Acad. Sci. U.S.A. **100**, 5449 (2003).
[7] H. C. Berg, *Random Walks in Biology* (Princeton University Press, Princeton, NJ, 1993).
[8] R. A. Arkowitz, Trends Cell Biol. **9**, 20 (1999).
[9] J. E. Segall, Proc. Natl. Acad. Sci. U.S.A. **90**, 8332 (1993).
[10] S. H. Zigmond, J. Cell Biol. **75**, 606 (1977).
[11] H. C. Berg and E. T. Purcell, Biophys. J. **20**, 193 (1977).
[12] W. Bialek and S. Setayeshgar, Proc. Natl. Acad. Sci. U.S.A. **102**, 10040 (2005).
[13] W. Rappel and H. Levine, Proc. Natl. Acad. Sci. U.S.A. **105**, 19270 (2008).
[14] W. J. Rappel and H. Levine, Phys. Rev. Lett. **100**, 228101 (2008).
[15] K. Wang, W. J. Rappel, R. Kerr, and H. Levine, Phys. Rev. E

75, 061905 (2007).
[16] R. G. Endres and N. S. Wingreen, Proc. Natl. Acad. Sci. U.S.A. **105**, 15749 (2008).
[17] S. Mukherjee, R. N. Ghosh, and F. R. Maxfield, Physiol. Rev. **77**, 759 (1997).
[18] S. S. F. Ferguson, Pharmacol. Rev. **53**, 1 (2001).
[19] R. Kubo, Rep. Prog. Phys. **29**, 255 (1966).
[20] R. G. Endres and N. S. Wingreen, Prog. Biophys. Mol. Biol. **100**, 33 (2009).
[21] L. F. Cugliandolo, J. Kurchan, and L. Peliti, Phys. Rev. E **55**, 3898 (1997).
[22] Th. M. Nieuwenhuizen, Phys. Rev. Lett. **80**, 5580 (1998).
[23] A. Crisanti and F. Ritort, J. Phys. A **36**, R181 (2003).
[24] L. Leuzzi, J. Non-Cryst. Solids **355**, 686 (2009).
[25] T. Lu, J. Hasty, and P. G. Wolynes, Biophys. J. **91**, 84 (2006).
[26] R. G. Endres and N. S. Wingreen, Phys. Rev. Lett. **103**, 158101 (2009).
[27] J. L. Rifkin, Cell Motil. Cytoskeleton **48**, 121 (2001).
[28] F. Kesbeke *et al.*, J. Cell. Sci. **96**, 668 (1990).
[29] C. M. Paulos *et al.*, Mol. Pharmacol. **66**, 1406 (2004).
[30] M. J. Catarina, D. Hereld, and P. N. Devreteos, J. Biol. Chem. **270**, 4418 (1995).
[31] H. Shankaran, H. Resat, and H. S. Wiley, PLOS Comput. Biol. **3**, e101 (2007).
[32] A. Bianco *et al.*, Nature (London) **448**, 362 (2007).
[33] P. Duchek and P. Rorth, Science **291**, 131 (2001).
[34] S. G. Nandini-Kishore and W. A. Frazier, Proc. Natl. Acad. Sci. U.S.A. **78**, 7299 (1981).
[35] S. K. Raths, F. Naider, and J. M. Becker, J. Biol. Chem. **263**, 17333 (1988).
[36] T. Yi, H. Kitano, and M. I. Simon, Proc. Natl. Acad. Sci. U.S.A. **100**, 10764 (2003).
[37] D. D. Jenness, A. C. Burkholder, and L. H. Hartwell, Mol. Cell. Biol. **6**, 318 (1986).
[38] L. Hicke, B. Zanolari, and H. Riezman, J. Cell Biol. **141**, 349 (1998).
[39] T. A. Nielsen, D. A. Di Gregorio, and R. A. Silver, Neuron **42**, 757 (2004).
[40] U. Olgac, V. Kurtcuoglu, and D. Poulikakos, Am. J. Physiol. Heart Circ. Physiol. **294**, H909 (2008); R. C. Roberts, D. G. Makey, and U. S. Seal, J. Biol. Chem. **241**, 4907 (1966); R. G. Thorne, S. Hrabetova, and C. Nicholson, J. Neurophysiol. **92**, 3471 (2004).
[41] J. E. Segall *et al.*, J. Cell. Sci. **91**, 479 (1998).
[42] A. Levitzki, *Receptors: A Quantitative Approach* (Benjamin, New York, 1984).
[43] L. Opresko and H. S. Wiley, J. Biol. Chem. **262**, 4109 (1987).
[44] K. A. Schandel and D. D. Jenness, Mol. Cell. Biol. **14**, 7245 (1994).
[45] K. J. Blumer and J. Thonnes, Proc. Natl. Acad. Sci. U.S.A. **87**, 4363 (1990).
[46] K. Kawada *et al.*, Mol. Cell. Biol. **29**, 4508 (2009).
[47] S. Minina, M. Reichman-Fried, and E. Raz, Curr. Biol. **17**, 1164 (2007).
[48] G. Jèkely, H. Sung, C. M. Luque, and P. Rorth, Dev. Cell **9**, 197 (2005).
[49] C. Le Roy and J. L. Wrana, Dev. Cell **9**, 167 (2005).
[50] S. R. Yu *et al.*, Nature (London) **461**, 533 (2009).
[51] I. Mellman, Annu. Rev. Cell Dev. Biol. **12**, 575 (1996).
[52] J. B. Hicks and I. Herskowitz, Nature (London) **260**, 246 (1976).
[53] N. Barkai, M. D. Rose, and N. S. Wingreen, Nature (London) **396**, 422 (1998).
[54] D. Choquet and A. Triller, Nat. Rev. Neurosci. **4**, 251 (2003).
[55] G. Aquino and R. G. Endres (unpublished).
[56] P. Detwiler *et al.*, Biophys. J. **79**, 2801 (2000).
[57] M. Thattai and A. van Ondenaarden, Biophys. J. **82**, 2943 (2002).
[58] G. Tkačik and W. Bialek, Phys. Rev. E **79**, 051901 (2009).